Proceedings World Geothermal Congress 2020+1
Reykjavik, Iceland, April - October 2021

Techno Economic Evaluation of Soft-Stimulation Measures Under Consideration of Uncertainty

Sören Welter, Elif Kaymakci, Dorothee Siefert, Thomas Kölbel

Durlacher Allee 93, D-76131 Karlsruhe

s.welter@enbw.com, e.kaymakci@enbw.com, d.siefert@enbw.com, t.koelbel@enbw.com

Keywords: techno-economic evaluation, uncertainty, risk factors, Monte-Carlo-simulation

ABSTRACT

The EU H2020 project DESTRESS shall demonstrate the application of stimulation techniques in different plays. The overall goal is an improvement of hydraulic reservoir parameters with minimal impact on environment and residents. Besides the applied research the investigation of risk factors as well as the economic effect of soft stimulation is a part of the DESTRESS project. The paper at hand presents the integration of uncertainty in general and uncertainty caused by risk factors in particular, which is a further development step in the techno-economic evaluation of geothermal power. Risk mitigation is an important part of risk management. Therefore, mitigation measures and the evaluation of mitigation measures are analyzed. Another subject of the study at hand is the presentation and application of developments in techno-economic modelling. Part of this is the usage of the Monte Carlo method for the investigation of uncertainty and for power plant optimization. For the main sub-models: reservoir, thermal fluid cycle and heat or power plant, respectively considerable evolution steps are presented. This includes e.g. optimization by Monte-Carlo-simulation, shell-and-tube heat exchangers or the adaption of economic correlations. The model and development steps are explained and applied to three selected demonstration sites. The aim is to demonstrate the "integrated geothermal energy model" (IGEM) and evaluate soft stimulation measures including uncertainty caused by risk factors. On the example of the Soultz-sous-Forêts site, the possibilities and first results of power plant optimization with the Monte-Carlo approach are demonstrated. A heat plant in Mezöberény (Hungary) is used to show the enhancement of hydraulic parameters through a stimulation and their effect on selected key performance indicators. The paper is concluded with a comparison of pure electricity provision and combined heat and power (CHP) on the example of a fictitious site in the Upper Rhine Graben (Germany).

1. INTRODUCTION

The Enhanced geothermal system (EGS) approach allows the usage of geothermal reservoirs that can't be exploited under the naturally given techno-economic frame conditions. Low hydraulic conductivities prevent an enormous potential of renewable energy to be used. Therefore, EGS measures aim to improve the productivity of a geothermal reservoir by increasing the hydraulic conductivity of the reservoir. Despite the great potential of EGS, the technology hasn't reached a wide diffusion in the market due to social, economic and environmental reasons. The DESTRESS project has the overall goal to investigate, improve and demonstrate the application of the EGS-approach. Within DESTRESS the idea of soft stimulation is put forward. Soft stimulation is a collective term for geothermal reservoir stimulation techniques that aim to increase reservoir performance while minimizing environmental impacts including the risk posed by induced seismicity. Soft stimulation includes techniques such as cyclic/fatigue stimulation multi-stage stimulation, chemical stimulation and thermal stimulation. The developments achieved in DESTRESS shall be demonstrated considering the site-specific geological requirements. The soft stimulation approach can be considered as an evolution step of the EGS approach. Thereby three overall goals shall be followed (Figure 1).

Figure 1: DESTRESS overall goals for the demonstration of stimulation activities

Techno-economic evaluation already plays an important role in guiding resources in an early research/demonstration phase. Common cost accounting models for business case calculations are insufficient to reflect the characteristics of geothermal energy production, therefore specialized models were developed by e.g. Beckers and McCabe (2019), Schlagermann (2014) or Welter (2018). Complex connections between technical and economic parameters in geothermal energy systems make a detailed techno-economic modelling necessary. Welter (2018) showed such interactions inter alia on the example of the temperature of the thermal water at the output of the power plant as presented in Figure 2. For the results presented in Figure 2 Welter (2018) investigated the case of a geothermal power plant in the Upper Rhine Graben (Germany) with a flow rate of 85 l/s (for further background information please refer to Welter (2018)). The thermal water temperature at the output of the power plant is determined by the energy usage in the power plant. It directly influences the physical properties (e.g. density) of the thermal water and thereby the hydraulic processes in the reservoir during injection which can be expressed in pumping power demand. The energy usage in the power plant as well as the hydraulics during injection have an economic impact by their influence on the sizing of the components and technically through the gross power and the parasitic power demand. All aspects are merged in the levelized costs of electricity.

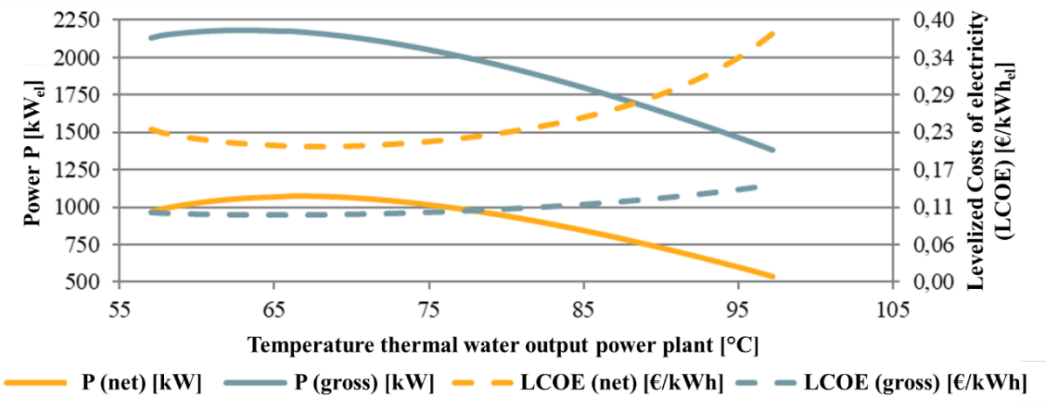

Figure 2: Dependency of power and levelized costs of energy from the output temperature of the thermal water at the power plant Welter (2018) [Geothermal power plant; Upper Rhine Graben; Germany; 85 l/s]

While techno-economic interdependencies as shown in Figure 2 are already part of ongoing research in geothermal energy utilization, the influence of uncertainty hasn't been investigated in the same depth. In other fields of underground usage e.g. CO_2-storage (see Bos and Wilschut (2013)) or even more the E&P industry the investigation of uncertainty is more elaborated. On the background of techno-economic modelling, uncertainty is mainly related to the realization of model parameters. Including the term risk, the parameters showing an uncertainty on their realization can be described as risk factors. Bos and Wilschut (2013) define risk as "probability of an undesired impact multiplied by the magnitude of that undesired impact" and risk factors as "model input parameter that have a high potential impact on risk".

Different risk factors are inherent to geothermal energy usage. The geological risk, as an example, causes challenges on the techno-economic evaluation of geothermal projects. Key technical data especially on underground topics can vary widely and are often poorly characterized in early project phases. Welter (2018) showed on an example in German Upper Rhine Graben, that the effect of risk factors on techno-economic results can be considerable. Welter (2018) investigated risk factors mainly related to the drilling process. Figure 3 shows that based on ten risk factors, the bandwidth between min. and max. values for techno-economic key performance indicators (KPI) can be as high as 200%. This clearly points out the importance of a further investigation of techno-economic evaluation in geothermal energy utilization under consideration of uncertainty also caused by risk factors.

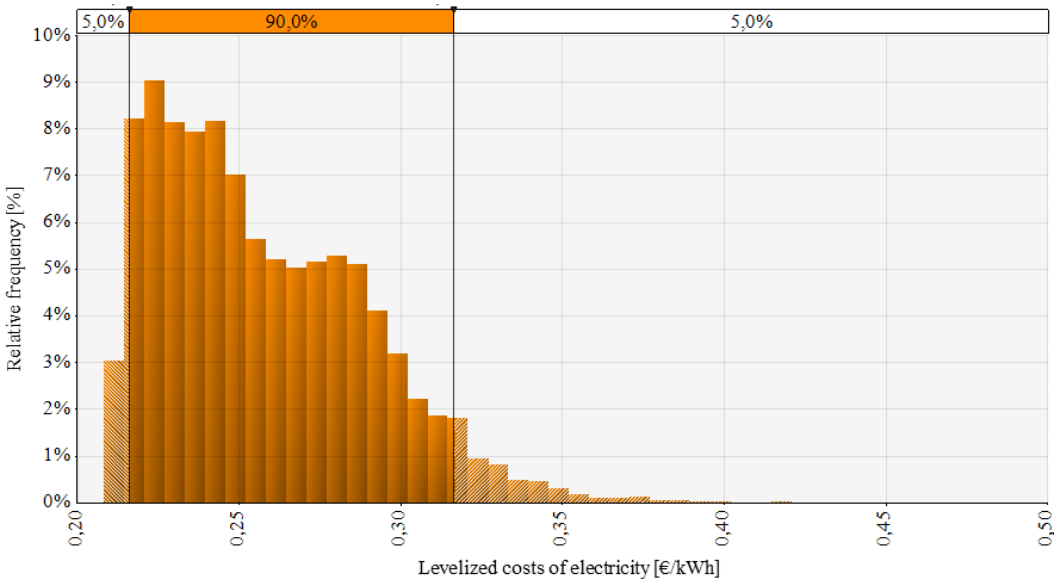

Figure 3: Effect of risk factors on the techno-economic results of a geothermal power plant in the Upper Rhine Graben, Germany Welter (2018)

Within the DESTRESS project existing approaches in techno-economic modelling were further developed. To deal with the uncertainty caused by risk factors, experiences from the E&P industries are applied by developing and using a Monte Carlo (MC) based techno-economic model. The necessary probability distributions and cost data are taken from publications of the DESTRESS project: Reith et al (2017), Welter et al. (2019a) and Welter et al (2019b). Another field of research in the DESTRESS project is the assessment of the latest geothermal power production technologies. Especially the most recent approaches on optimizing Organic Rankine Cycles was investigated. The access to very detailed data of geothermal power plants in operation made an in-deep validation possible, which is another strength of the presented model. Further effort is spent on the adaption of the MC based cost calculation model on regional markets. For the evaluation of geothermal projects, the common accounting KPI such as internal rate of return (IRR), net present value (NPV) and levelized cost of energy (LCOE) are introduced. Furthermore, multi-use cases were mapped in detail in the presented model. Most other renewables are incapable of directly providing heat, geothermal is particularly

suited to district heating or combined heat and power (CHP) application. To demonstrate the economic and environmental benefits of heat and combined heat and power (CHP) provision, these usage pathways of geothermal energy are also mapped in the model.

2. PROGRESS IN TECHNO-ECONOMIC MODELLING (IGEM)

2.1. Integrated geothermal model

The IGEM in its current development status is based on the techno-economic model used in Welter (2018) and has been further developed by the DESTRESS-partners University of Glasgow (UoG), Netherlands organization for applied scientific research (TNO) and Energie Baden-Württemberg (EnBW). In the following a brief introduction shall be given. For further information, please refer to Welter et al. (2019b).

The IGEM consists of several sub models that are merged through a model backbone. One of the central development approaches of the IGEM is the usage of Monte-Carlo-Simulations. The "Monte Carlo Method" is a powerful approach to solve problems, where analytical approaches fail or can only be implemented with considerable effort. It is used in diverse scientific disciplines for quantitative analysis. The basis of this approach is formed by many similar random experiments. The goal is the analysis of the system behaviour in the random experiments. Monte-Carlo-Simulations are often used to integrate uncertainty into models. The uncertainty is integrated through parameters/risk factors (see definition above). In addition, the paper at hand also documents new approaches in power plant modelling. While Welter (2018) used a heuristic optimization for the identification of an optimized power plant design, the IGEM uses a Monte-Carlo-approach for the optimization of power plant designs. The heuristic optimization used in Welter (2018) limited the solution space by changing only one parameter in a defined step size. The power plant modelling presented in this paper manipulates five central parameters at different state points of the power plant. This increases the solution space and the optimal solution can be better approximated. IGEM is using the Monte-Carlo approach on two different topics that are statistically independent. The integration of uncertainty, mainly caused by risk factors, as well as the simulation and optimization of power plants designs. While both fields are methodologically integrated in the main model, they are technically separated in the actual code to limit the computational effort. The power plant modelling is outsourced from the main model. Based on a set of deterministic, technical input parameters, the Monte-Carlo-Simulation for the power plant is done before running the main model. The results (multiple deterministic power plant designs) are stored in a database and can be accessed by the main model through a function defined by a parameter set. For more details on the structure and modelling approaches of the IGEM, please refer to Welter et al. (2019b). In the following specific evolution steps of the IGEM over its previous versions are described.

2.2. Power plant optimization by Monte-Carlo-Simulation

In this chapter, the technical sub-model is described, considering all possible uses of geothermal energy. A single-stage Organic-Rankine-Cycle (ORC) plant is modelled. In addition to the pure provision of electricity, the simultaneous provision of electricity and heat (CHP - combined heat and power) are studied. For CHP, three circuit variants are being investigated. Heat extraction can be connected in parallel or in series, or a combination of both, Eyerer et al. (2017). The wiring diagram of the system is shown in Figure 4.

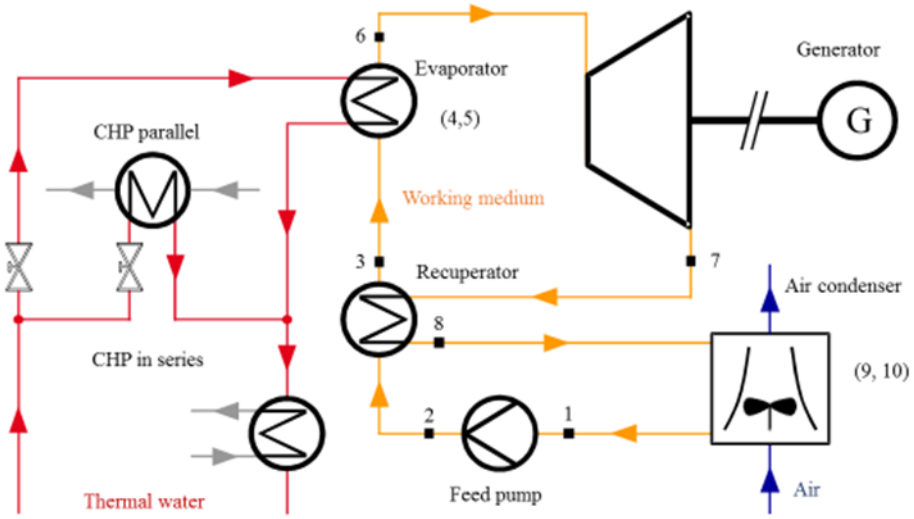

Figure 4: Schematic depiction of ORC with CHP Welter et al. (2019b)

The central element of the power plant is the clockwise working medium circuit, consisting of the components of working medium pump, optional recuperator, evaporator, turbine, generator and air condenser. Other condenser types are not considered. The state changes of the working medium between the state points entered in Figure 4 are determined in Matlab based on the REFPROP database, Lemmon et al (2018). These are described as key points below:

- $1 \rightarrow 2$: Pressure increase in feed pump
- $2 \rightarrow 3$: Heat supply in recuperator
- $3 \rightarrow 4$: Pre-heating to boiling point in evaporator
- $4 \rightarrow 5$: Complete evaporation in evaporator
- $5 \rightarrow 6$: Overheating in evaporator

- $6 \rightarrow 7$: Decompression in turbine
- $7 \rightarrow 8$: Heat removal in recuperator
- $8 \rightarrow 9$: Pre-cooling to dew point in condenser
- $9 \rightarrow 10$: Complete condensation in condenser
- $10 \rightarrow 1$: Undercooling in condenser (not considered in this work)

The site-specific data such as flow rate, temperature, pressure and salinity of the geothermal fluid are defined externally. Furthermore, the parameters to be varied within the Monte-Carlo simulation and their upper and lower limits are determined in Table 1. A certain number of Monte Carlo iterations are then run through to simulate many different power plant designs. Thereby temperatures, enthalpies and entropies of the working medium for the ten defined state points shown in Figure 4 are determined using REFPROP, Lemmon et al. (2018). The selected pressures and pressure losses in the system determine the pressure at the respective point of state before and after the feed pump. In all heat exchangers a pressure drop of 2% is assumed, Chacartegui et al. (2009). Within the same routine, feed pump and turbine are modelled with a firmly defined isentropic efficiency of 80%, respectively 85%. As a value of motor and generator an efficiency of 96% is assumed, Schlagermann (2014). The generator also has a gearbox, the efficiency of which is approximated to be 98%, Welter (2018).

Table 1: Overview Monte-Carlo parameters power plant Welter et al. (2019b)

Parameter	Upper limit	Lower limit
p_1	$0{,}5p_2$	$p(X=0, T_{air,in})$
p_1	If $T_{TW,in} - \Delta T^{min} < T_{crit} - \Delta T^{min}$ $p(X=1, T=T_{TW,in} - \Delta T^{min})$ Else $p(X=1, T=T_{crit} - \Delta T^{min})$	$1{,}5p_1$
$0T_6$	$T_{TW,in} - \Delta T^{min}$	$T(X=1, p_2 * \zeta_{evap} * \zeta_{cond})$
$\Delta h_{7,8}$	Pinch-analysis	$0kJ/kg$
$T_{TW,out}$	$T_{TW,in} - 50K$	$55°C$

The heat exchangers are considered in more detail to calculate the required heat exchanger area. The evaporator, condenser, recuperator and the heat exchanger or exchangers for heat extraction at CHP are simplified and modelled as shell-and-tube heat exchangers (SHE), which are operated in counter-current mode. Whether and to what extent a recuperator is installed in the system is randomly varied in the Monte-Carlo simulation. If the decision is made in favor of a recuperator, the working medium cycle, initially evaluated without such a recuperator, is modified using the "recuperator quick" routine.

2.3. Representation of tube heat exchangers in techno-economic modelling

In past studies e.g. Schlagermann (2014), Welter (2018) tube heat exchangers were described as very relevant in practical application but not modelled because of complexity. This gap between operational reality and simulation model is closed by the IGEM. Figure 5 presents a sketch of a tube heat exchanger showing the input variables for the Matlab routine.

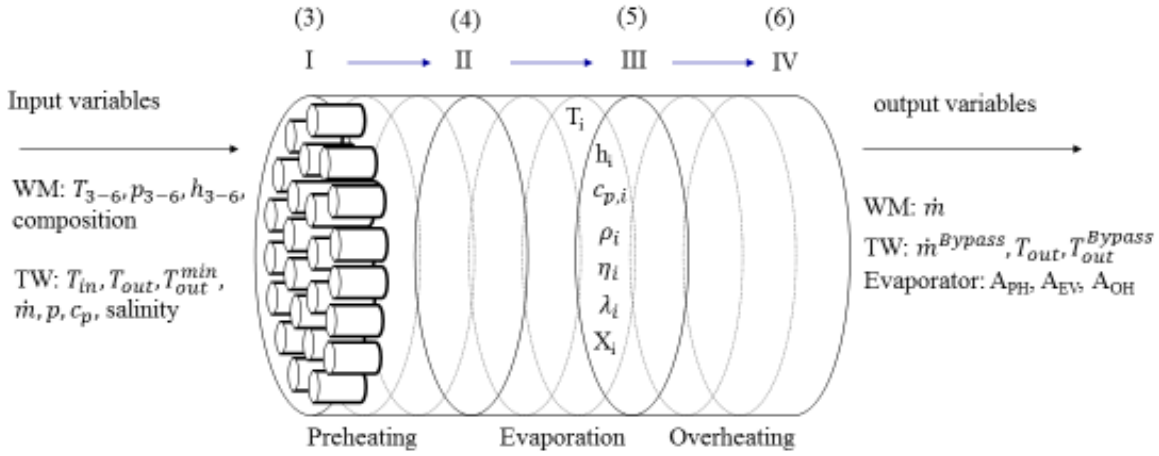

Figure 5: Schematic depiction of tube heat exchanger with in- and output parameters Welter et al. (2019b)

Pressure, temperature and enthalpy of the working medium at the state points of the ORC are required, as well as the working medium composition and properties of the thermal water at the power plant entrance. Furthermore, the minimum permissible

temperature of the thermal water after the evaporator must be known, which is defined by the lower limit of the Monte Carlo parameter $T_{TW,\,in}$. In addition, Figure 5 shows the output variables of the routine. These are the heat transfer surfaces for preheating (A_{PH}), evaporation (A_{EV}) and overheating (A_{OH}) and the working medium mass flow. Another output is the maximum thermal water mass flow required for combined heat and power generation in parallel connection (bypass) in the present design of the ORC, which can be routed past the evaporator. The last output value represents the temperature of the thermal water after the evaporator for both cases with and without heat extraction in parallel. For all calculations, the specific heat capacity of the thermal water $c_{p,TW}$ is assumed to be constant over the considered temperature and pressure range. The admissibility of this simplification is demonstrated in Welter (2018). The aim is to determine the working medium mass flow, the maximum recuperable bypass mass flow and the outlet temperature of the thermal water at the maximum bypass mass flow rate while maintaining the minimum temperature difference ΔT^{min} at each point in the evaporator. First, it is assumed that the entire available thermal water mass flow is led through the evaporator and that the entire extractable heat is transferred to the working medium flow. This allows to determine the maximum working medium mass flow with equation (1).

$$\dot{m}_{WM} = \frac{\dot{m}_{TW} * (T_{TW,IV} - T_{TW,I}) * c_{p,TW}}{h_{WM,IV} - h_{WM,I}} \quad \textbf{(1)}$$

In this equation, $\dot{m}$ stands for the mass flow, T for the temperature, c_p for the heat capacity, and h for the enthalpy. The WM and TW indices represent working fluid and thermal water. The enthalpy $h_{WM,I}$ is the enthalpy of the working medium at the temperature at state point I($T_{TW,I}$). The heat exchanger area of each individual section (i) can be calculated using equation (2). The calculation procedure is based on the approach presented in Heberle & Brüggemann (2016) and Welter (2018).

$$A_i = \frac{\dot{m}_{WM} * (h_{WM,i+1}^{edge} - h_{WM,i}^{edge})}{k_i * \Delta T_i^{ln}} \quad \textbf{(2)}$$

The working medium mass flow $\dot{m}_{WM}$ is known from the calculations above. The specific enthalpies $h_{WM,i+1}^{edge}$ and $h_{WM,i}^{edge}$ are the left and right boundary values of the subsection and thus taken from the NIST database according to Lemmon, et al. (2018). k_i stands for the overall heat transfer coefficient of the subsection. The logarithmic temperature difference ΔT_i^{ln} between hot and cold current for each range from the temperatures of the working medium and thermal water are calculated at the edges of the subsections.

To determine the condenser surface areas, considerations must be made to maintain the minimum temperature difference, like the evaporator. Since the working medium mass flow is already known from the evaporator routine, the procedure is simplified. In principle, the heat transfer from the working medium flow to the air flow in the condenser is also considered based on the Pinch method, Kemp (2007) and is therefore not explained in detail here. The condenser surface areas and the fan power are determined. The latter is calculated according to equation (3).

$$P_{Fan} = \frac{\dot{m}_{Air} * \Delta p_{Fan}}{\rho_{Air} * \eta_{Fan}} \quad \textbf{(3)}$$

To calculate the fan power, 100 Pa is assumed for the pressure increase Δp_{Fan} by the fan and 70% for the total fan efficiency η_{Fan}. The values are derived from manufacturer data by Systemair (2018) and a valid EU directive EU (2009). Furthermore, the density of the air is approximated with the value at ambient pressure and inlet temperature. In the recuperator routine, the heat exchanger area is determined from the temperatures, pressures and enthalpies at state points 2, 3, 7 and 8, as well as the composition of the working medium. For the calculation of the evaporator, based on the “pinch method”, Kemp (2007), the recuperator state points are already examined. All in all, the recuperator model is a simplified version of the evaporator or condenser model.

2.4. Reduction of computation time for enabling the Monte-Carlo approach

Within the power plant design, many technical parameters must be defined for the design of the individual components and their interaction in the ORC. Almost all process parameters of the ORC have not only technical but also economic consequences, i.e. they influence not only the performance of the system but also its price. Therefore, the selection of an ORC system that is technically and economically optimal is a complex task and the exact numerical solution requires a great deal of effort. This subject is addressed in the present study with the help of the Monte Carlo method. The Monte Carlo method is a powerful tool for solving problems where analytical approaches fail or can only be implemented with considerable effort. It is used for quantitative analysis in various scientific disciplines. The basis for this is many similar random experiments. The aim is the analysis of the system behavior in random experiments. From the results obtained, conclusions can be drawn about the real system behavior, Dunn & Shultis (2011). If the method is used in a simulation, the term Monte Carlo simulation is used Dunn & Schultis (2011). A downside of the Monte-Carlo approach is the high demand of computation time. To enable a realistic computation time, a lot of effort was spent on efficient coding and reducing computation time.

Altogether, the generation of many different concrete design options replaces a numerical optimization of the ORC. If enough different possibilities are considered, a design, which is sufficiently close to the actual optimal solution, can be assumed. An exact determination of the necessary number of iterations to determine the optimal power plant design in accordance with the electricity generation costs is not possible. Methods such as those described by Driels & Shin (2004) refer to the determination of the number of iterations necessary for the mean value of the results of a Monte-Carlo-simulation to be sufficiently close to the mean value of the same Monte Carlo simulation with an infinite number of repetitions. In the present case, however, no expected value for the electricity production costs is sought, but rather the technically and economically optimal power plant design. For the application in the DESTRESS research project, the model is also intended for estimating electricity production costs in early phases of project development in the corporate environment and must therefore deliver results in a limited time. For this reason, the number of evaluated power plant designs is set to 1000, accepting that the global optimum is only approximated.

2.5. Adapted pump technology - Line shaft pump (LSP)

Another development compared to the technical model in Welter (2018) is on the production pump. For geothermal plays in central Europe, artesian outflow often doesn't provide sufficient flow rate, therefore a production pump has to be installed. Two technical solutions are on the market. In the past only electrical submersible pumps (ESP) were considered in techno-economic, whereas line shaft pumps (LSP) showed increasing relevance especially in the Upper Rhine Graben. For the determination of the temperature increase by friction losses within the production pump, a distinction is made between submersible pump (ESP, equation (4)) and line shaft pump (LSP, equation (5)). With ESP, the engine is in the wellbore and is surrounded by thermal water. Heat losses from the engine are therefore transferred to the geothermal fluid, Francke (2014). The engine of the LSP, on the other hand, is located above ground and the resulting heat is not transferred to the thermal water or only to a negligible extent.

$$\Delta T_{loss}^{ESP} = \frac{\Delta p_{pump} * (1-\eta_{is} * \eta_{mot})}{\rho_{TW} * c_{p,TW} * \eta_{is} * \eta_{mot}} \quad (4)$$

$$\Delta T_{loss}^{LSP} = \frac{\Delta p_{pump} * (1-\eta_{is})}{\rho_{TW} * c_{p,TW} * \eta_{is}} \quad (5)$$

Here η_{is} represents the isentropic efficiency and η_{mot} for the motor efficiency of the pump. The temperature difference calculated in this way is considered in the wellbore section in which the pump is installed. Like the specific heat capacity $c_{p,TW}$, the density of the thermal water ρ_{TW} is calculated as described in Francke (2014).

2.6. Temperature calculation-Ramey's approach

To determine the temperature of the thermal water in the well, knowledge of the well geometry is necessary as the diameter and angle of the well influence heat exchange with the environment. In addition, temperature calculations require information about the temperatures in the soil surrounding the hole. Both the geometry of the hole and the temperatures in the subsurface are specified by the user for the simulation. Figure 6a shows schematically a vertical and a deviated hole. Figure 6b shows a schematic representation of a section of a cemented wellbore.

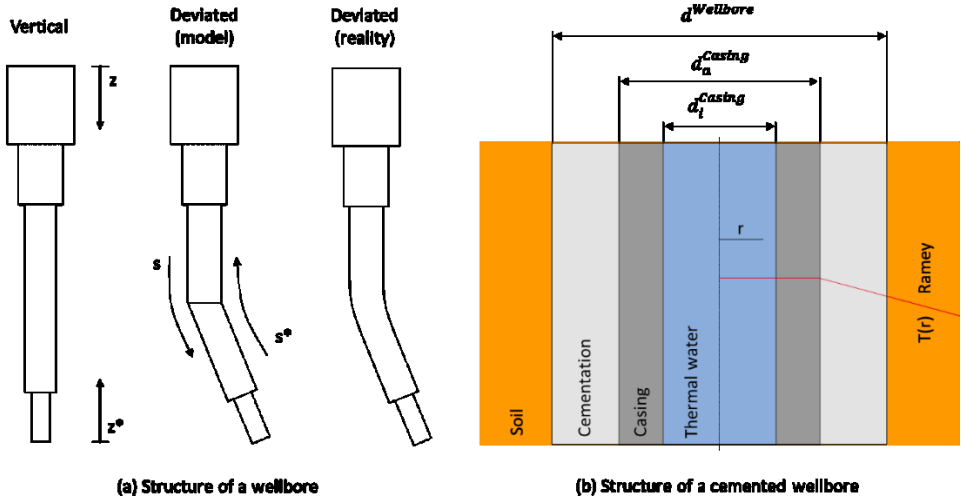

Figure 6: Schematic structure of production and injection wellbore Welter (2018)

The temperature of the thermal water at the outlet of each well section ($T_{TW,out}$) is determined based on the inlet temperature ($T_{TW,in}$) and the temperature difference as a result of the heat transfer (ΔT_{HE}) to the ground and, if applicable, the temperature difference ΔT_{pump} generated by the pump (equation (4); (5)). The latter is only included in the section in which the pump is installed.

$$T_{TW,out} = T_{TW,in} + \Delta T_{HE} + \Delta T_{pump} \quad (6)$$

For the determination of ΔT_{HE}, the approach presented by (Ramey, 1962) for determining the temperature profile of a fluid injected into a borehole is evaluated section by section. The expression used is shown in equation (7). In Welter (2018) the wells are simulated as a multi-layered hollow cylinder. This approach has a higher computational effort but didn't show a significant increase in accuracy that would justify the higher computation time.

$$\Delta T_{HE} = T_{TW,in} - \frac{dT_{geo}}{ds} * \Delta s - T_{geo}(z = z_{out}) + \frac{dT_{geo}}{ds} * F(t) - \left[T_{TW,in} + \frac{dT_{geo}}{ds} - T_{geo}(z = z_{out})\right] * e^{\frac{-\Delta s}{F(t)}} \quad (7)$$

ΔT_{TW} represents the change of the thermal water temperature over a section depending on the measured depth (MD) s and the observation time t. The latter is the time elapsed between the start of production of geothermal fluids and the observation time of the stationary state depicted in the simulation. In Ramey (1962), a value of 30 days is set for the observation period. T_{geo} describes the temperature in the rock surrounding the borehole. The gradient of this temperature in z-direction is assumed to be constant in sections in this paper. z_{out} symbolizes the depth at which the outlet of the respective section is located. For the application to geothermal energy wells, however, the thermal resistance within the borehole can be neglected, Ramey (1962). This simplification

corresponds to the assumption that the temperature in thermal water and piping is the same in the stationary state. Furthermore, the cementation is neglected and its thermal conductivity with that of the surrounding rock. The associated idealized temperature profile is shown in Figure 6. Under this assumption $F(t)$, a time function, is calculated according to context (8).

$$F(t) = \frac{\dot{m}_{TW} * c_{p,TW} * f(t)}{2 * \pi * \lambda_{geo}} \quad \textbf{(8)}$$

For the still unknown time function f(t) Ramey (1962) uses the equation for transient heat conduction of a line source in an infinite radial system (equation (9)).

$$f(t) = -ln\left(\frac{d_a^{casing}}{4 * \sqrt{a_{geo} * t}}\right) - 0{,}29 + \frac{\left(a_a^{casing}\right)^2}{4 * a_{geo} * t} \quad \textbf{(9)}$$

Using expression (6), the thermal water temperature at each outlet can be determined for each section of the injection well. Equation (6) can be applied in the same form to the production well if the measured depth (MD) s is substituted by the measured distance from reservoir s* (see Figure 6a). Haagort (2004) describes the Ramey (1962) approach as "excellent approximation after a short transient period during which the temperature is overestimated". Ramey (1962) gives a duration of about 7 days after which this period ends. Beckers K. J. (2016) also uses the Ramey (1962) approach, which proves its continuing relevance.

2.7. Economic model

Within the technical sub-models, all system properties required for economic evaluation are determined and passed on to the corresponding economic sub-models. In the power plant model, for example, the heat exchanger surfaces and component power are relevant for cost estimation. Within the economic sub-models, the investment and operating costs of the power plant, thermal water cycle and reservoir are determined. With the help of these costs and the technical properties of the system, the “Levelized costs of electricity” (LCOE) are calculated and used for the technical-economic evaluation of the overall system. The calculation of the net electricity production costs enables an economic comparison of different types of electricity generation technologies, IEA; NEA; OECD (2015). The LCOE are calculated according to equation (10).

$$\mathbf{LCOE_{net}} = \frac{\mathbf{I_0 + Z + \sum_t^{tmax} (1+i)^{-t} * (C_{Operation} - R)}}{\mathbf{\sum_t^{tmax} (1+i)^{-t} * \tau v * P_{el,net}}} \quad \textbf{(10)}$$

I_0 stands for the investment costs and Z the interest during the construction period. Due to the time lag between the start of the construction and the commissioning of the power plant, the investment costs are incurred before the start of the period under consideration (t_{max}). They are referenced to the beginning of the period under consideration by means of the construction period interest rate Z. The calculatory interest rate i of 7%, including income taxes, is estimated using the method of Konstantin (2017). For a detailed description of this procedure, see Welter (2018). $C_{Operation}$ describes the operating costs in relation to an operating year, R characterizes the heat revenue from cogeneration. Furthermore, v symbolizes the annual full load hours for power generation at the power plant and $P_{el,net}$ its net electrical output, meaning the power fed into the grid minus its own consumption. Besides LCOE also other key performance indicators (KPI) are implemented in the IGEM. As shown in Figure 14, internal rate of return (IRR) and net present value (NPV) are also calculated by the model. The mentioned KPIs share most of the input parameters and can be derived from each other. While LCOE has a specific energy price as output, IRR and NPV need it is input. Assumptions on energy prices are explained in detail in Welter et al. (2019b).

The investment costs are calculated using the module costing technique (MCT), which was originally developed for estimating the costs of chemical plants, Turton et al. (2013). The method is also widely used for energy plants, such as ORC plants in Welter (2018), Schlagermann (2014), Astolfi (2014), Collings et al. (2016), Wang et al. (2015) and Toffolo et al. (2014). The module costing method is not used to calculate the price of the components of the thermal water circuit, due to the lack of suitable correlations. Instead, correlations according to Welter (2018) and Schlagermann (2014) are used to determine the various cost items. In the course of DESTRESS the existing cost engineering approaches were updated by recent literature findings. Besides this general revision of the economic model, a special focus is put on the approaches for stimulation costs and the line shaft pump, as these correlations didn’t receive much attention in techno-economic modelling for geothermal energy systems, yet.

2.7.1. Cost of stimulation measures

A widely used approach to define cost functions is a regression analysis. In a retro perspective functions/approaches are developed that can incorporate historical data points. In the DESTRESS project, Reith et al. (2017) presented cost functions based on the experience of projects in France. Additional data points to enhance the cost functions will be collected in the further course of the DESTRESS project, after the soft stimulation approach has been applied at different sites.

2.7.2. Cost of line shaft pumps

A downhole geothermal Line Shaft Pump is a vertical centrifugal pump driven by a motor installed on surface through a shaft. The wide use of LSP in water wells became possible after the development and adaption of an oil lubrication system for LSP. Currently, there are about 190 downhole geothermal LSP in operation in California, Nevada, Utah and Idaho, and very few pumps in the rest of the world (Germany, France, Japan and Mexico), Frost (2010). The first oil lubricated downhole geothermal LSP in Europe was put in operation in 2007 in Landau, followed in 2012 in Insheim and in 2016 in Rittershoffen and Soultz-sous-Forêts. Some experiences with Icelandic LSP were carried out at Soultz-sous-Forêts from 2008 to 2012 but with a very limited success, Ravier, Graf, & Villadangos (2015).

Capital expenditure related to LSP were investigated within DESTRESS. CAPEX in € for such pump installed in Europe was estimated in the following equation (11) using the rule of six-tenths. In this formula, CAPEX includes strainer, pump, lubstring, production column, wellhead discharge, wellhead thermal compensator, surface pump supporting, electrical motor, frequency driver, lubrication system and connection, installation preparation, installation at depth and start-up. In equation (11) z is the setting depth in meters and P_{hydro} the hydraulic power of the pump in kW.

$$\mathbf{CAPEX}(\mathbf{z}, \mathbf{P_{hydro}}) = \mathbf{470000} + \mathbf{700} \times \boldsymbol{z} + \mathbf{225000} \times \left(\frac{\boldsymbol{P_{hydro}}}{\mathbf{450}}\right)^{\mathbf{0.67}} \quad \textbf{(11)}$$

Electrical consumption is the main operating cost position. After nearly 3 years of operation, overall efficiency of the LSP installed at Rittershoffen geothermal site, including the electrical motor and surface cables, can be calculated to 70%. Other operating costs are related to oil bearing consumption and maintenance of surface equipment. Annual oil consumption for the lubrication of the bearings is about 40 barrels per year, which is recovered regular. The oil for lubrication represents an operational expenditure of nearly 16 k€ per year including oil recycling. During geothermal plant shut down every 4 months, motor and lineshaft must be uncoupled and coupled during start-up procedure. Therefore, crane and maintenance operations are required, representing about 6 k€ per shut down over 1 day. The surface mechanical seal must be replaced every two years, which costs about 6 k€ for the spare part. Bearings of the electrical motor also must be replaced every 5 years during a long shut down period. The costs of such an operation sum up to nearly 15 k€, Welter et al. (2019b). Based on this data, annual OPEX of downhole geothermal LSP can be estimated with the equation (12). Where z is the setting depth in meters and P_{hydro} the hydraulic power of the pump in kW.

$$\boldsymbol{OPEX}\left(\boldsymbol{T_{operating}}, \boldsymbol{P_{elec}}, \boldsymbol{P_{hydro}}\right) = \frac{\boldsymbol{P_{hydro}}}{\mathbf{0.7}} \times \boldsymbol{P_{elec}} \times \boldsymbol{T_{operating}} + \mathbf{28000}€ \quad \textbf{(12)}$$

2.8. Risk Factors as a source of uncertainty

Risk factors can have a generic character like accidents or delays, they can be linked to certain operations like the handling of hazardous goods during a chemical stimulation but can also be site specific like the effect of local geology on operations. The focus of this paper is the evaluation of soft stimulation measures in general, therefore the risk analysis takes the same focus and investigates only the uncertainties caused by risk factors directly associated with the stimulation measures and site-specific effects shall not be included in the investigations.

2.8.1. Effect of stimulation measures on reservoir performance

To evaluate the effect of stimulation measures, a literature review on published data for stimulation activities is conducted. In total, data on 136 geothermal stimulation jobs conducted since 1970 in 15 countries is acquired. Figure 7 shows the relative improvement achieved by the different stimulation jobs, including chemical, hydraulic and thermal stimulation techniques. The relative improvement shows a wide range depending on technical and geological issues. The expectation value of improvement of the considered jobs is 314 %. 84 % of all cases show an improvement, whereby 75 % show an improvement larger than 23 %.

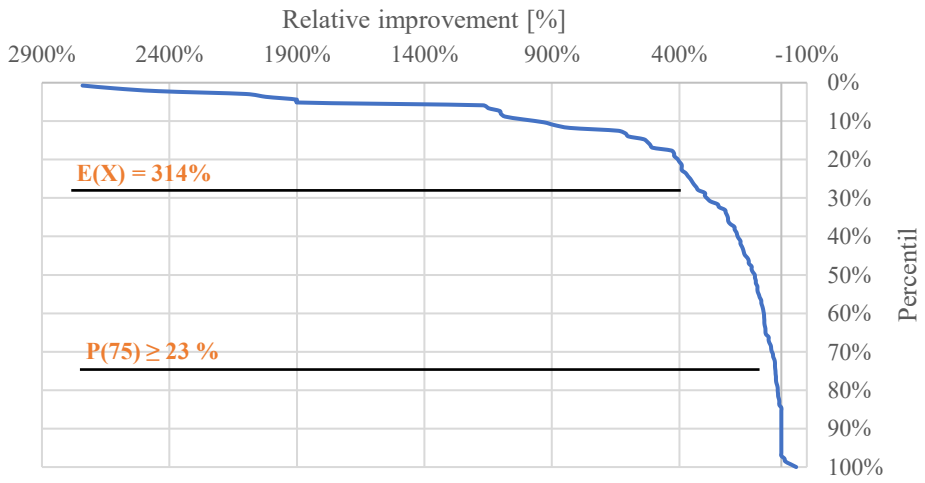

Figure 7: Relative improvement through stimulation Welter et al. (2019b)

2.8.2. Integration of risk factors

In this study, the ten most important risk factors identified by Reith, et al. (2017) are implemented. Table 2 provides an overview of the risk factors considered. It describes the model parameters influenced in each case as well as the effect in the negative scenario estimated by expert interviews, published in Reith et al. (2017), and the probability of occurrence of this negative scenario. The following two assumptions are made for all risk factors (6 to 8 in Table 2) that affect the permeability of the reservoir: First, the individual changes in permeability add up to a total change. And secondly, the individual deviations and the cumulative change of the permeability is such that the reservoir permeability decreases maximum an order of magnitude based on its initial value.

Table 2: Parameters for the integration of risk factors in techno-economic modelling Welter et al. (2019b)

	Risk factor	Influenced Parameter	Effect	Probability	σ
1	Public Acceptance	Investment Public Acceptance	660'000 €	8,2%	380'000 €
2	Lack of information	Investment Exploration	260'000 €	6,4%	140'000 €
3	Induced seismicity (with time delay after injection)	Investment Public Acceptance	1'400'000 €	1,6%	600'000 €
4	Change in legislations	Investment Planning	2'300'000 €	2,0%	1'000'000 €
5	Induced seismicity exceeding threshold	Investment Public Acceptance	1'000'000 €	1,6%	420'000 €
6	Loss of effectivity	Permeability Reservoir	Decrease to 10%	2,0%	Depends on location
7	Fluid-rock interactions	Permeability Reservoir	Decrease to 10%	1,7%	Depends on location
8	Fluid-fluid interactions (thermal brine and chemicals)	Permeability Reservoir	Decrease to 10%	1,7%	Depends on location
9	Political Instability	Investment Planning (III)	2'300'000 €	1,2%	930'000 €
10	Lost in hole (measuring tool)	Investment Reservoir (V)	2'300'000 €	1,3%	940'000 €

By means of effect and probability of occurrence the standard deviation of the semi-normal distribution is estimated through the sigma level. The probability of occurrence given by Reith et al. (2017) is translated as the probability that the effect of each risk factor will be at least equal to or greater than the effect given in Table 2. For further insight into the modelling of risk factors please refer to Welter et al. (2019b).

3. APPLICATION OF THE IGM TO DESTRESS SITES

Chapter 2 presents the integrated geothermal energy model. In the following, the IGEM is applied to selected demonstration sites of the DESTRESS project. On the example of Soultz-sous-Forêts (France) the developments in simulating power generation are presented. As a second site, the geothermal power plant of Mezöberény (Hungary) was selected. Due to the relatively low reservoir temperature of approximately 100 °C, the site is used for the demonstration of the effect of stimulation on flow rate in a geothermal heat plant. None of the DESTRESS demonstration site plans or operates a CHP unit. But as pointed out e.g. by Welter (2018), CHP can considerably improve the profitability of geothermal power utilization. Therefore, CHP is implemented in the IGEM and is presented on a fictive location in the German part of the Upper Rhine Graben. On the example of the case studies, different functionalities of the IGEM will be presented together with the deduction of general results on soft stimulation and power plant modelling. An overview of all site-dependent model parameters can be found in the Appendix. Monte Carlo simulations are a major development step of the presented IGEM. The required number of Monte Carlo iterations was determined using a methodology described by Driels and Shin (2004). According to the methodology of Driels and Shin (2004) 150 Monte Carlo iterations are needed for the case studies of the Soultz-sous-Forêts and Upper Rhine Graben sites. For the Mezöberény site 250 iterations are needed.

Heat can only be distributed locally. Therefore, the demand side plays an important role in investigating CHP plants. For the heat demand two different operating cases are evaluated. First, a base load operation of the CHP plant is investigated. In this case only maintenance and repair work are taken into account as down time, which leads to about 8000 annual full load hours of the heat and power unit. It is assumed that the total heat generated from CHP will be supplied to a customer. Second, a heat-controlled operation of the CHP plant is considered. A defined heat requirement is covered as much as possible by the geothermal plant. The heat demand is specified in the form of an annual duration curve, which is formed according to the methodology of Sochinsky, Blesl et al. (2009). Energy not needed for the satisfaction of the heat demand is transformed to electricity. It is assumed that the ORC power plant can be operated up to a minimum partial load of 25% without changing the individual state points. Under these conditions, the thermal water mass flow used by the power plant is assumed to be directly proportional to the working fluid mass. If the working fluid mass flow is reduced to 25% of the nominal mass flow, the required thermal water mass flow is also reduced to 25% of the thermal water mass flow in nominal operation. Thereby, not only the rated thermal nominal output of the power plant but also a range of thermal outputs is available to cover the heat demand profile. The nominal mass flows result from the power plant design. When designing the power plant and CHP components, the described mass flow shift is considered. The heat demand that cannot be covered by the mass flow shift is provided by a boiler. Based on these assumptions, the electrical energy produced can be determined from the heat duration curve.

3.1. Developments in power plant simulation on the example of the Soultz-sous-Forêts geothermal site

The Soultz-sous-Forêts geothermal project started in 1987 and is the cradle of the European research on harvesting geothermal energy in granitic and fractured systems. All over all five wells were drilled for research purposes at the site. Besides stimulation

techniques, corrosion, scaling, power plant technique but also questions concerning the operation of a geothermal power plants were investigated by a group of international researchers. After almost 30 years of research, the geothermal site is exploiting the fractured basement at 5 km depth, under commercial conditions. Since June 2016 a new ORC-power plant with isobutane as working medium is operated with a gross power of 1.7 MW_{el}. The geothermal loop is composed of one production well GPK-2 and two reinjection wells GPK-3 and GPK-4. After the electricity production the geothermal brine is fully reinjected at around 70 °C without using reinjection pumps, Mouchot et al (2019). Below 4.5 km the reservoir is made of crystalline basement and underwent various kinds of hydraulic and chemical stimulations together with several periods of long-term circulations, Schill et al. (2017). Although GPK-2 is an artesian well, the production of geothermal brine is enhanced by a line shaft pump to around 30 l/s. The reservoir temperature is slightly above 200 °C but the geothermal brine is produced with a temperature of 150 °C, Baujard et al. (2018). Since commissioning the power plant, between June and August 2016, the overall system showed outstanding availabilities. The total plant availability developed from 90% in 2017 to 95.9% in 2018. The net efficiency of the ORC plant was 11.5 % in 2017. In that year the gross electrical production was nearly 9,7 GWh and the total electrical consumption, including ORC auxiliaries and production pump, was around 3,7 GWh, resulting in an overall net electrical production for the whole plant of 5,9 GWh. These figures varied only slightly for 2018, Mouchot et al (2019). The model input data used for the simulation results presented in the following is derived from real-world operation conditions (see Table 3 in the Appendix). The technical (triplet) and economic (former research facility) frame conditions at the Soultz-sous-Forêts site make a model-like depiction of the real-world conditions very complicated. Therefore, the absolute values of the economic KPIs shown in the following don't replicate the reality. Nevertheless, the technical results show a good match and general recommendations can be derived.

The Monte-Carlo-simulation approach in power plant modelling is one of the major development steps towards existing geothermal techno-economic models. The investigation of sensitivities in power plant modelling opens new possibilities for the optimization of geothermal electricity provision. Figure 8 below displays pressure after the feed-pump over LCOE. By applying the Monte-Carlo-approach, pressure after feed-pump is manipulated. The results presented in Figure 8 clearly point out, that the operation of the power plant on a high-pressure level has a positive impact on LCOE. Compared to Figure 8, Figure 9 doesn't show such a clear correlation. The temperature of the working medium after overheating doesn't seem to be one of the main steering parameters for the LCOE. Two local optima could be assumed at 130 °C and 150 °C. But there are also data-points with considerably higher and lower temperatures, that show low LCOE.

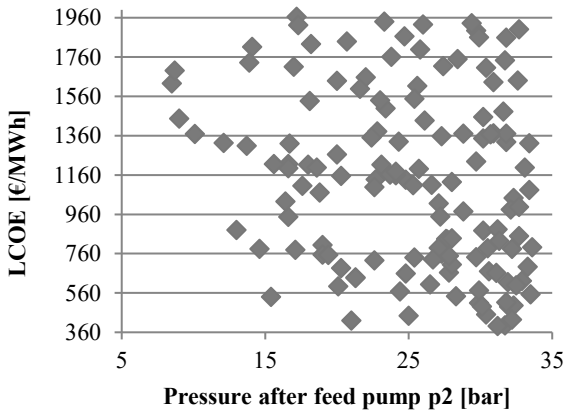

Figure 8: Power plant modelling: LCOE over pressure after feed-pump (Pure electricity; LSP; $\dot{m} = 33\ kg/s$; 150 Monte-Carlo iterations; 1000 power plant configurations; working medium isobutene; chemical stimulation; including risk factors; without risk mitigation measures)

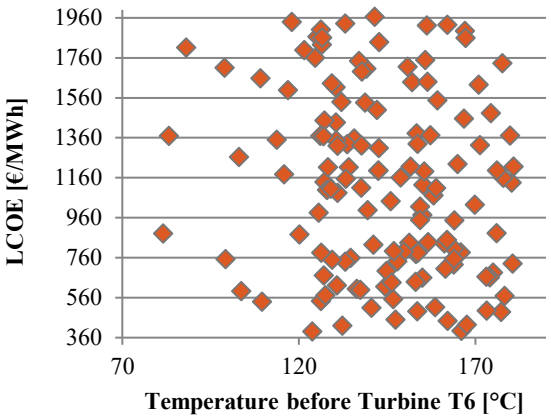

Figure 9: Power plant modelling: LCOE over temperature after overheating (Pure electricity; LSP; $\dot{m} = 33\ kg/s$; 150 Monte-Carlo iterations; 1000 power plant configurations; working medium isobutene; chemical stimulation; including risk factors; without risk mitigation measures)

When investigating the absolute overheating in Figure 10 the deduction of a clear correlation is difficult. Over a wide temperature range of around 60 K low LCOE values are reached. These results suggest, that overheating has no direct impact on LCOE and therefore doesn't have to be investigated in further detail. While the influence of overheating on LCOE isn't clear, on a technical level clear connection can be drawn as Figure 11 shows. With a rising thermal water outlet temperature the net power of the overall power plant (including all auxiliaries e.g. production pump) clearly decreases as can be seen in Figure 11.

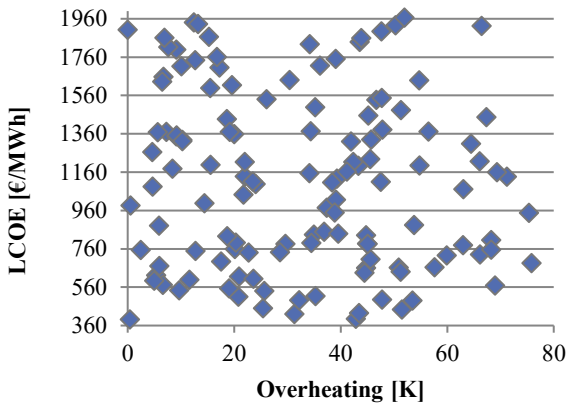

Figure 10: Power plant modelling: LCOE over overheating (Pure electricity; LSP; $\dot{m} = 33\ kg/s$; 150 Monte-Carlo iterations; 1000 power plant configurations; working medium isobutene; chemical stimulation; including risk factors; without risk mitigation measures)

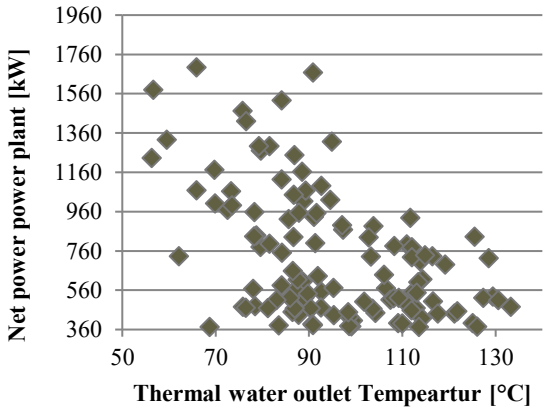

Figure 11: Power plant modelling: Net power over thermal water output temperature (Pure electricity; LSP; $\dot{m} = 33\ kg/s$; 150 Monte-Carlo iterations; 1000 power plant configurations; working medium isobutene; chemical stimulation; including risk factors; without risk mitigation measures)

3.2. Effect of stimulation on the example of heat provision at the geothermal site in Mezöberény (Hungary)

The Mezöberény geothermal site is situated in the Pannonian basin. Through a rolling back subduction, the basement was pulled off the basin. Thereby the thickness of the crust was reduced, which brings the hot asthenosphere closer to the surface and creates a heat anomaly. A mean heat flow density of 90-100 mW/m2, and an average geothermal gradient of 45 °C/km was published by Royden, Horvath, & Buchfiel (1982) for the Pannonian basin. The reservoir has an average permeability of 500-1500 mD with a bulk porosity of 20-30 %. While generally a uniform hydrostatic pressure distribution can be expected, local changes through recharge and discharge have to be expected, Tóth A. (2012), Dövényi et al. (1983). Between 2011 and 2012 the Mezöberény geothermal site was constructed. The goal was to power a geothermal heating system with geothermal water from the Békés Basin. The production well was planned to exploit the higher upper Pannonian sandstones of the Zagyva Formation, due to a poor sandstone formation with low productivity the production well was deepened to the Ujfalu-Formation, Siklósi (2017). The injection well was drilled to the same depth to inject into the same reservoir. The doublet with a depth of 2000 m was put into service in August 2012. After a short time of operation the injectivity dropped dramatically and the plant was stopped due to injectivity problems. A chemical and mechanical cleaning was performed in 2017, which had the goal to remove the clogging of the downhole filters. Since then no long-term operation has taken place, Siklósi (2017). Table 4 (see Annex) summarizes the modelling input parameters of the Mezöberény power plant.

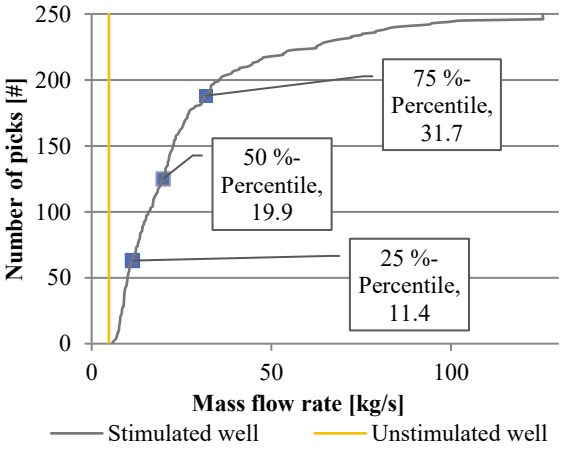

Figure 12: Effect of stimulation for the Mezöberény site (250 Monte-Carlo iterations; chemical stimulation; including risk factors; without risk mitigation measures)

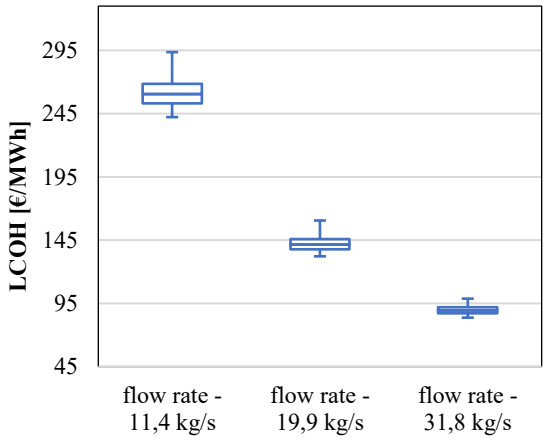

Figure 13: Effect of increased flow rate on techno-economic performance (Pure heat provision; baseload; ESP; 250 Monte-Carlo iterations; chemical stimulation; including risk factors; without risk mitigation measures)

As explained above, poor hydraulic properties of the Mezöberény wellbores adversely affect the economic operation of the project. The soft stimulation approach investigated in DESTRESS aims to enhance the hydraulic conditions of a site with minimum impact on the environment and people. On the example of the Mezöberény site, it shall be demonstrated which impact a stimulation could have on the techno-economic performance of a site. The risk factors presented in chapter 2.8 are included in the simulation as well as the risk mitigation measures. All other frame conditions are kept constant with respect to the base-case presented in Table 4.

Figure 12 shows the effect of stimulation, simulated for the Mezöberény site according to the literature data presented in chapter 2.8. Besides the simulated results of the soft stimulation job, the original flow rate as well as the 25%-, 50%- and 75%-percentile of the distribution are plotted. As discussed in Welter et al. (2019b) the effect of stimulation depends on multiple frame conditions of geological, geophysical and chemical nature. Therefore and because of the limited data availability, the presented results should be interpreted conservative. The techno-economic evaluation of the stimulation effect is presented in Figure 13. The presented box plots give the median of the distribution (horizontal line in the middle of the box), the 75%-percentile (upper limit of the box), the 25%-percentile (lower limit of the box) and the Minimum/Maximum of the distribution shown by the whiskers. With an increase of flow rate a decrease of the LCOH can be observed. This effect was expected. Components with a high investment, e.g. wellbores, are not sensitive to the flow rate, so that the produced energy escalates quicker with the growing flow rate than the costs do. More important for the evaluation of uncertainty is that the width of the distribution is reduced with an increase of flow rate. Caused by the bigger amount of produced energy, the impact of single cost categories and the uncertainty on them is reduced. This example demonstrates, that the "economies of scale", already investigated in Welter (2018), not only show a positive effect on techno-economic KPIs but also reduce the impact of uncertainty.

3.3. Evaluation of CHP on the example of a fictive geothermal power plant in the Upper Rhine Graben (Germany)

None of the DESTRESS demonstration sites operates or plans a CHP-plant. Therefore, to demonstrate the CHP functionality of the IGEM and show the effect of CHP, a fictitious example is created. The site shall be located on the German side of the Upper Rhine Graben. The input data presented in Table 5, is fictitious but based on expert knowledge. It is assumed that two deviated boreholes explore the Buntsandstein in a depth of 3600 m. Through its favorable conditions with a reservoir temperature of 160 °C and a pumped flow rate of 120 kg/s the site can be used for all types of energy provision. It is also assumed that access to a heat network with unlimited demand exists.

Heat and electricity have a different exergy level. Therefore, the techno-economic comparison of pure electricity provision and CHP is challenging from a methodological point of view. To solve this question, heat is assessed with a heat price and integrated into the LCOE calculations as revenues, IEA; NEA; OECD (2015). This approach causes a sensitivity of the evaluation results to the heat price, which was investigated e.g. by Welter (2018). Beside LCOE also IRR and NPV are investigated in this paper. Both KPIs integrate the different energy streams by monetary values. For the results presented in Figure 14, a heat price is derived by taking 50% of the household gas price in the investigated country. In contrast to heat, renewable electricity in Germany is supported by a subsidiary system guaranteed by the "Erneuerbaren Energie Gesetz" (EEG), which is simplified in this study to a feed-in-tariff. Under these assumptions, a fixed remuneration of 252 €/MWh for 20 years is assumed, BMWi (2018). As the period of observation in this study is 30 years the remaining time is evaluated with 100 €/MWh according to Capros, et al. (2016). Figure 14 shows the results of a comparison between pure electricity provision and CHP at the fictitious site "Upper Rhine Graben". The Assessment is based on IRR and LCOE. These KPI are drawn on the ordinate, while on the abscissa, the investigated power plant configurations are pictured, so that the most economic power plant configuration can be identified. The Monte-Carlo-Simulation of the power plant generates a defined number of randomly sampled configurations. The optimality of configurations are evaluated on low LCOE, high IRR, or high NPV. The presented power plant configurations are selected by having an IRR > 1% and sorted in descending order subject to their IRR.

For CHP only 6 out of 1000 power plant configurations fulfill the selection criteria, while at least 34 out of 1000 power plant configurations for pure electricity provision, have an IRR >1. This suggests that with the given assumptions on market prices, pure electricity provision should be preferred as it is less sensitive to a non-optimal power plant configuration/operation. This finding contradicts the studies presented by Schlagermann (2014) and Welter (2018). Both studies investigated CHP and saw an advantage over pure electricity provision. Both evaluated geothermal CHP on the basis of LCOE as KPI. Based on LCOE, the results presented in Figure 14 are consistent with other studies, as half of the presented CHP configurations show lower LCOE than the best pure electricity configuration. The apparent contradiction between LCOE and the other KPI can be explained on a methodological basis. While LCOE-calculations have the energy price as a result, IRR and NPV have it as an input parameter. Given the frame conditions of this simulation with subsidies included, apparently contradicting results can be explained. This illustrates the macro-economic character of LCOE as KPI, while NPV and IRR rather have a micro-economic focus. It can be summarized that under the given frame conditions power plants with pure electricity provision show higher IRRs compared to CHP. Nevertheless, CHP power plants also can generate interesting IRRs with over 7%. Additionally, it was shown that a purely technical optimization is not constructive for an investor (see Appendix A4).

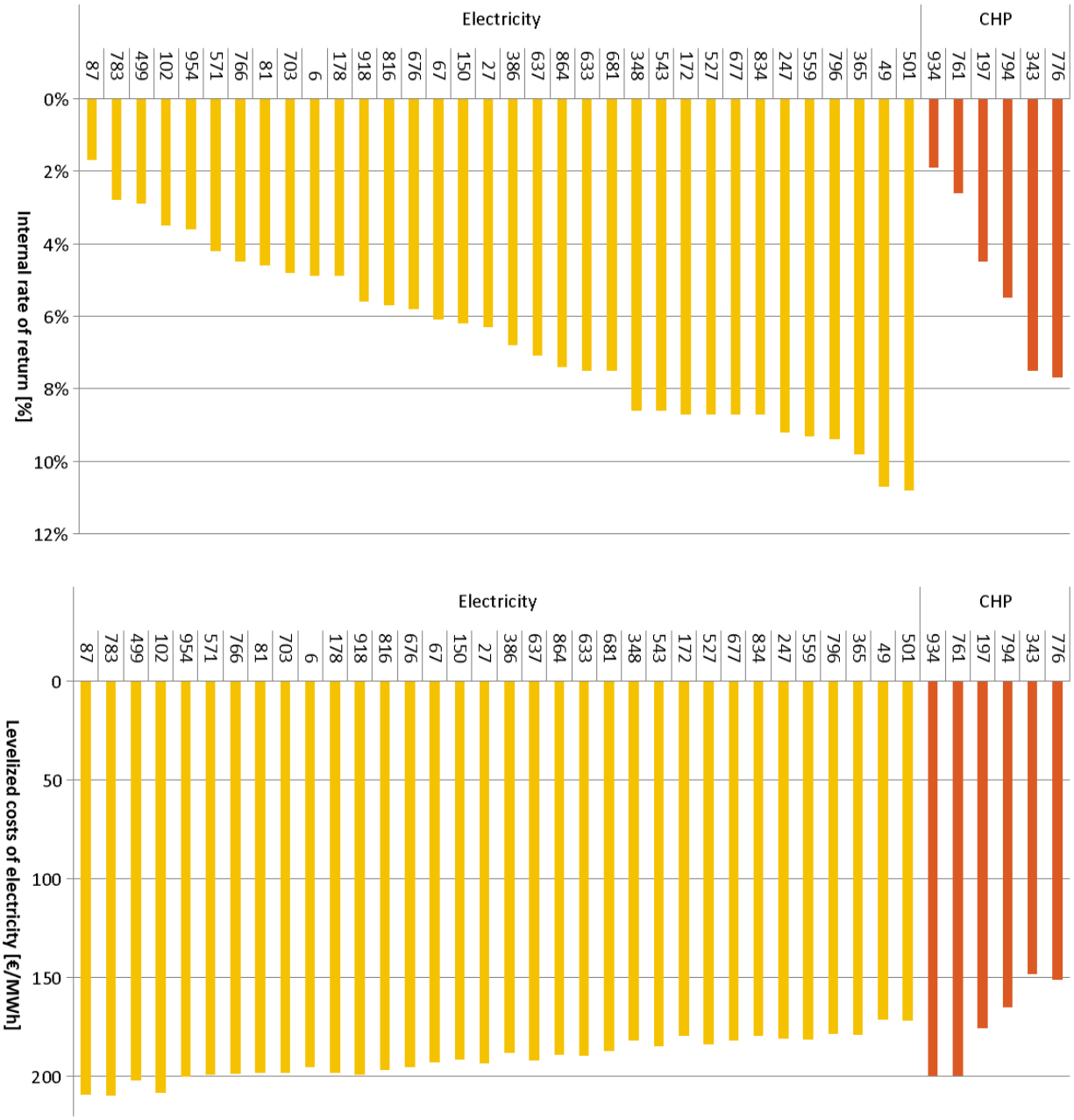

Figure 14: Comparison of pure electricity provision and CHP based on IRR and LCOE (Pure electricity/CHP provision with parallel setup; baseload; ESP; $\dot{m} = 120\ kg/s$; 150 Monte-Carlo iterations; 1000 power plant configurations; hydraulic stimulation; including risk factors; with risk mitigation measures)

4. CONCLUSION

The overall goal of the presented research is to improve techno-economic evaluation of geothermal energy provision. Besides pure modelling and simulation issues, improvements in techno-economic evaluation also arise from the methodological approach of decision analysis that forms the methodological background of this research (see Welter et al. (2019b)). With this methodological backbone, uncertainty can be integrated into techno-economic modelling. Thereby risk factors, and the uncertainty that comes with them, is included in the Integrated geothermal energy model (IGEM).

The IGEM includes the results published in Reith et al. (2017) and also features considerable improvements compared to the first development step of the IGEM presented in Welter (2018): Uncertainty accompanies the evaluation of a project over all life cycle steps. In the early phase of project development there is considerable uncertainty on frame conditions, while during the realization, risk factors can affect the project. Therefore, uncertainties regarding both technical and economic model parameters are considered and quantified using the Monte-Carl method. Ten different risk factors are currently implemented. Due to the modular structure of the IGEM, additional risk factors can be easily incorporated. Another significant improvement was possible in terms of technical modelling. While in Welter (2018) the Organic Rankine Cycle was calculated with a heuristic optimization approach, the current version of the IGEM optimizes the power plant with the Monte Carlo method. A basis for this step is the model presented in (Collings, et al., 2016). This new approach enlarges the solution space and thereby improves the quality of optimization. In addition to this methodological improvement also the mapping of technical features is improved. The introduction of pinch analysis

in all heat exchangers guarantees physically consistent power plant designs in this model. In addition, shell-and-tube heat exchangers are introduced, which corresponds to the state of the art for geothermal applications. In addition, combined heat and power provision already presented in Welter (2018) is implemented into the Monte-Carlo simulation of the power plant and enriched with the possibility of simulating pure heat generation. In general, the model is improved in its structure and has more efficient algorithms in all model parts compared to its first evolution step. This enables the computation-intensive Monte Carlo simulation to quantify the influence of various risk factors while maintaining reasonable calculation times. In addition to the improvements in the technical models and the program code, the economic model part is also improved. While maintaining the general structure selected correlations are updated to map the reality more closely. Supplementary to the adaption of single parameters in existing correlations, completely new cost functions are introduced. As an example, the representation of LSP and the updated stimulation cost functions can be named. Another important step to meet the demand of DESTRESS is an adaption of the geographical focus of the cost engineering sub-models, which now maps all European countries. The development of a model is a huge task but becomes meaningless if the reality can't be mapped with good accordance, which is another major strength of the IGEM. The technical as well as the economic sub-models are validated with extraordinary detailed insight into operational and economic data of running geothermal power plants. This step lays the foundation for the significance of the IGEM.

Although the results of a techno-economic evaluation are always site specific, the presented examples show interesting results that can be used to derive general statements:

- Under the conditions of the Soultz-sous-Forêts site with a relatively high wellhead temperature, low flow rate and isobutane as working fluid, operation conditions can be deduced. While a high operational pressure in the working medium cycle and a low thermal water output temperature have a positive impact on the LCOE, the overheating doesn't show a clearly positive impact.
- On the Mezöberény case it was possible to show that with an increase of produced energy, the width of the distribution of results is reduced. Bigger projects therefore can cope with a negative realization of single uncertain parameters more easily.
- The comparison of CHP and pure electricity provision on the example of the fictitious Upper Rhine case, didn't only show the importance of using different KPI for the techno-economic evaluation, but also the need for a purpose tailored technical configuration of geothermal power/heat plants.

ACKNOWLEDGEMENT

The DESTRESS project is funded by the European Commission's Horizon 2020 Research and Innovation Programme under grant agreement No 691728. This work was also supported by the New and Renewable Energy Technology Development Program of the Korea Institute of Energy Technology Evaluation and Planning (KETEP) through a grant funded by the Korean Government's Ministry of Trade, Industry & Energy (No. 20123010110010), the National Research Foundation of Korea (NRF) through a grant (No. NRF-2015K1A3A7A03074226) funded by the Korean Government's Ministry of Science and ICT, and the Swiss State Secretariat for Education, Research and Innovation (SERI).

REFERENCES

Astolfi, M. (2014). An Innovative Approach for the Techno-Economic Optimization of Organic Rankine Cycles. Mailand: PhD thesis, Politecnico di Milano.

Averfalk, H., & Werner, S.: Essential improvements in future district heating systems. Energy Procedia 116, pp. 217 - 225. (2017).

Baujard, C., Genter, A., Cuenot, N., Mouchot, J., Maurer, V., Hehn, R., Vidal, J.: Experience learnt form a succesfull soft stimulation and operational feedback after 2 years of geothermal power and heat production in Rittershofen and Soultz-sous-Forêts plants (Alsace, France). Geothermal Resource Council, GRC2018, (pp. 2241 - 2263). Reno. (2018).

Beckers, K. J. (2016). Low-Temperature Geothermal Energy: Systems Modeling, Reservoir Simulation, and Economic Analysis. Cornell: Cornell university.

Beckers, K. F. and McCabe, K.: Geophires v2.0: Updated geothermal techno-economic simulation tool, Geothermal Energy, 7:5, (2019).

Blesl, M., Kempe, S., Ohl, M., Fahl, U., König , A., Jenssen, T., & Eltrop, L.: Wärmeatlas Baden-Württemberg: Erstellung eines Leitfadens und Umsetzung für Modellregionen. . Stuttgart: Institut für Energiewirtschaft und Rationelle Energieanwendung (IER) Universität Stuttgart. (2009).

BMWi: Erneuerbare-Energien-Gesetz vom 21. Juli 2014 (BGBl. I S. 1066), das zuletzt durch Artikel 1 des Gesetzes vom 17. Dezember 2018 (BGBl. I S. 2549) geändert worden ist. (2018).

Bos, C. F. M.; Wilschut, F.: Assessing the uncertainty in the performance predictions of natural subsurface systems that are used for CO2 storage. ULTimateCO2 - Deliverable D6.1. Utrecht. (2013).

Brandt, W.: Training course on geothermal electricity, session v: Drilling. GEOELEC training course. Potsdam: German research center for geoscience. (2013).

Capros, P., De Vita, A., Tasios, N., Siskos, P., Kannavou, M., Petropoulos, A., . . . Kesting, M.: EU Reference Scenario 2016 - Energy, transport and GHG emissions - Trends to 2050. Bruxelles: European Comission. (2016).

Chacartegui, R., Sanchez, D., Munoz, J., & Sanchez, T.: Alternative orc bottoming cycles for combined cycle power plants. Applied Energy 86, pp. 2162-2170. (2009).

Collings, P., Yu, Z., & Wang, E. (2016). A dynamic Organic Rankine Cycle usting a zeotropic mixture as the working fluid with composition tuning to match changeing ambient conditions. Applied Energy 171, pp. 581-591.

Dövényi, P., Horváth, F., Liebe , P., Gálfi, J., & Erki, I.: Geothermal conditions of Hungary. Geophysical Transactions, pp. 3-114. (1983).

Driels, R., & Shin, S. Y.: Determining the number of iterations for monte carlo simulations of weapon effectiveness. Naval Postgraduate School. (2004).

Dunn, W. L., & Shultis, J. K. (2011). Exploring Monte Carlo Methods. Amsterdam: Elsevier.

EU: Richtlinie 2009/125EG des Europäischen Parlaments und des Rates vom 21. Oktober 2009 zur Schaffung eines Rahmens für die Festlegung von Anforderungen an die umweltgerechte Gestaltung energieverbrauchsrelevanter Produkte. Amtsblatt der Europäischen Union. (2009).

EUROSTAT: Retrieved from http://ec.europa.eu/eurostat/web/products-datasets/-nrg_pc_203. (2018, May 29).

Guth, A.: Monte-Carlo-Simulation der Stromgestehungskosten im Oberrheingraben. Karlsruhe: Energie Baden-Württemberg AG; Karlsruher Institute of Technology. (2011).

Eppelbaum, L., Kutasov, I., & Pilchin, A.: *Applied Geothermics.* Berlin: Springer Vieweg. (2014).

Eyerer, S., Schifflechner, C., Hofbauer, S., Wieland, C., Zosseder, K., Bauer, W., Spliethoff, H. (2017). Potential der hydrothermalen Geothermie zur Stromerzeugung in Deutschland. Geothermie-Allianz Bayer.

Francke, H. (2014). Thermo-hydraulic model of the two-phase flow in the brine circuit of a geothermal power plant. Berlin: Technische Universität Berlin.

Haagort, J. (2004). Ramey's wellbore heat transmission revisited. SPE Journal, pp. 465 - 474.

Heberle, F., & Brüggemann, D. (2016). Thermo-economic analysis of zeotropic mixtures and pure working fluids in organic rankine cycles for waste heat recovery. Energies 9, pp. 226-241.

Held, S., Genter, A., Kohl, T., Kölbel, T., Sausse, J., & Schoenball, M.: Economic evaluation of geothermal reservoir performance through modeling the complexity of the operating egs in soultz-sous-forêts. Geothermics 51, pp. 270 – 280. (2014).

IEA; NEA; OECD: International Energy Agency, Nuclear Energy Agency and Organisation for Economic Co-operation and Development: Projected costs of generating electricity. (2015).

Kemp, I. C. (2007). Pinch Analysis and Process Integration (Second Edition). Oxford: Butterworth-Heinemann.

Konstantin, P. (2017). Praxisbuch Energiewirtschaft. Springer Verlag.

Lemmon, E.W., Bell, I.H., Huber, M.L., McLinden, M.O. NIST Standard Reference Database 23: Reference Fluid Thermodynamic and Transport Properties-REFPROP, Version 10.0, National Institute of Standards and Technology, Standard Reference Data Program, Gaithersburg, 2018.

Mouchot, J., Ravier, G., Seibel, O., & Pratiwi, A.: Deep Geothermal Plants Operation in Upper Rhine Graben: Lessons Learned. European Geothermal Congress 2019. Den Haag: European geothermal energy council. (2019).

Mouchot, J., Genter, A., Cuenot, N., Scheiber, J., Seibel, O., Bosier, C., & Ravier, G.: First year of operation from EGS geothermal plants in alsace, france: Scaling issues. Proceedings, 43rd Workshop on Geothermal Reservoir Engineering. Stanford: Stanford University. (2018)

Ramey, H. J. (1962). Wellbore heat transmission. Journal of petroleum technology, 14, pp. 427 - 435.

Reith, S., Hehn, R., Mergner, H., & Kölbel, T.: Systematic preparation of the techno-economic evaluation of soft stimulation. Potsdam: DESTRESS research project. (2017).

Royden, L. H., Horvath, F., & Buchfiel, B.: Transform faulting, entension and subduction in the Carpathian Pannonian region. Geological society of America, pp. 717-725. (1982, August).

Scheiber, J.: Operation parameters for the Soutlz-sous-Forêts plant. (S. Welter, & C. Bormann, Interviewers). (2018).

Schill, E., Genter, A., Cuenot, N., & Kohl, T.: Hydraulic performance history at the Soultz EGS reservoirs from stimulation and long-term circulation tests. Geothermics 70, pp. 110 - 124. (2017).

Schlagermann, P.: Exergoökonomsiche Analyse geothermischer Strombereitstellung am Beispiel des Oberrheingrabens. PhD Thesis; Munich: Technische Universität München. (2014)

Seibel, O.: Operation data Soultz-sous-Forêts. (S. Welter, & C. Bormann, Interviewers) (2018).

Siklósi.: Internal report Mezöberény geothermal project (unpublished). (2017).

Systemair: *Ventilatoren und Zubehör (Katalog)*. Retrieved from https://www.systemair.com/de/Deutschland/Support/ (2018, 06 19).

Tóth, A.: Geothermal energy production and utilization in hungary. Geoscience and engineering, pp. 315-319. (2012).

Turton, R., Bailie, R. C., Whiting, W. B., Shaeiwitz, J. A., & Bhattacharyya, D.: Analysis, Synthesis, and Design of Chemical Processes. Pearson Education Inc. (2013).

Welter, S.: Technisch-ökonomische Analyse der Energiegewinnung aus Tiefengeothermie in Deutschland. PhD Thesis; Stuttgart: Universität Stuttgart. (2018)

Welter, S., Brehme, M., Nowak, K., Kaymakci, E., & Kölbel, T.: Identification and quantification of risk mitigation measures with respect to soft simulation technique based on relevant technical non-technical factors. Potsdam: DESTRESS research project. (2019a).

Welter, S., Bormann, C., Bos, C. F., Collings, P., Hehn, R., Guillaume, R., Kaymakci, E., Siefert, D., Kölbel, T., Förderer A., Seyfarth, R. Greve, J.: Key performance indicator analyses based on Monte Carlo simulation. Potsdam: DESTRESS research project. (2019b).

APPENDIX

A1. Model input parameters Soultz-sous-Forêts geothermal site

Table 3: Model input parameters Soultz-sous-Forêts geothermal site

	Parameter	Value/setting	Reference
Reservoir / Thermal water circuit	$p_{Reservoir}^{Production}$	50,0 MPa	Scheiber (2018)
	$p_{Reservoir}^{Injection}$	50,0 MPa	Scheiber (2018)
	$T_{Reservoir}^{Production}$	201 °C	Schill, Genter, Cuenot, & Kohl (2017)
	$T_{Reservoir}^{Injection}$	201 °C	Schill, Genter, Cuenot, & Kohl (2017)
	$h_{Thickness}^{Production}$	1000 m	Scheiber (2018)
	$h_{Thickness}^{Injection}$	1000 m	Scheiber (2018)
	$K^{Production}$	4*10^{-14} m²	Held et al. (2014)
	$K^{Injection}$	2*10^{-14} m²	Held et al.(2014)
	S	7,8*10^{-5}	Guth (2011)
	λ_{geo}	1,58 $W\ /\ mK$	Eppelbaum, Kutasov, & Pilchin (2014)
	a_{geo}	10,28*10^{-7} $m^2\ /\ s$	Eppelbaum, Kutasov, & Pilchin (2014)
	$z_{Production}$	5000 m	Mouchot et al. (2018)
	$z_{Injection}$	5000 m	Mouchot et al. (2018)
	Type well	Deviated	Brandt (2013)
	Type pump	LSP	Seibel (2018)
	R	700 m	Mouchot et al. (2018)
Power plant	$\dot{m}_{TW}$	33,3 $kg\ /\ s$	Seibel (2018)
	ΔT^{min}	5 K	Assumption
	$T_{air,in}$	15 °C	Assumption
	Working medium	Isobutane	Seibel (2018)
	$p_{TW,in}^{Heat\ plant}$	2,2 MPa	Seibel (2018)
CHP	T_{Flow}	70 °C	Averfalk & Werner (2017)
	$T_{Back\ flow}$	45 °C	Averfalk & Werner (2017)
	$p_{network}$	8 bar	Assumption

A2. Model input parameters Mezöberény geothermal site

Table 4: Model input parameters Mezöberény geothermal site

	Parameter	Value/setting	Reference
Reservoir / Thermal water circuit	$p_{Reservoir}^{Production}$	19,0 MPa	Geo-Log Kft. (2012)
	$p_{Reservoir}^{Injection}$	17,1 MPa	Geo-Log Kft. (2012)
	$T_{Reservoir}^{Production}$	80 °C	Geo-Log Kft. (2012)
	$T_{Reservoir}^{Injection}$	100 °C	Calculated according to temperature gradient
	$h_{Thickness}^{Production}$	400 m	Assumption
	$h_{Thickness}^{Injection}$	400 m	Assumption
	$K^{Production}$	9,5*10^{-14} m²	Geo-Log Kft. (2012)

	$K^{Injection}$	5,0*10^{-14} m²	Geo-Log Kft. (2012)
	S	7,8*10^{-5}	Geothermia Expressz Kft. (2016)
	λ_{geo}	1,58 $W\ /\ mK$	Eppelbaum, Kutasov, & Pilchin (2014)
	a_{geo}	10,28*10^{-7} $m^2\ /\ s$	Assumption
	$z_{Production}$	5000 m	Geo-Log Kft. (2012)
	$z_{Injection}$	5000 m	Geo-Log Kft. (2012)
	Type well	Vertical	Geothermia Expressz Kft. (2016)
	Type pump	ESP	Assumption
	R	1400 m	Geothermia Expressz Kft. (2016)
Heat plant	$\dot{m}_{TW}$	4,8 $kg\ /\ s$	Welter, Brehme, Nowak, Kaymakci, & Kölbel (2019)
	$p_{TW,in}^{Heat\ plant}$	2,2 MPa	Assumption
	T_{Flow}	70 °C	Averfalk & Werner (2017)
	$T_{Back\ flow}$	45 °C	Averfalk & Werner (2017)
	$p_{network}$	8 bar	Assumption

A3. Model input parameters Upper Rhine Graben geothermal site

Table 5: Model input parameters Upper Rhine Graben geothermal site

	Parameter	Value/setting	Reference
Reservoir / Thermal water circuit	$p_{Reservoir}^{Production}$	33,1 MPa	Assumption
	$p_{Reservoir}^{Injection}$	33,1 MPa	Assumption
	$T_{Reservoir}^{Production}$	160 °C	Assumption
	$T_{Reservoir}^{Injection}$	160 °C	Assumption
	$h_{Thickness}^{Production}$	420 m	Assumption
	$h_{Thickness}^{Injection}$	420 m	Assumption
	$K^{Production}$	1,43*10^{-13} m²	Assumption
	$K^{Injection}$	1,43*10^{-13} m²	Assumption
	S	1*10^{-8}	Assumption
	λ_{geo}	2,3 $W\ /\ mK$	Assumption
	a_{geo}	9*10^{-7} $m^2\ /\ s$	Assumption
	$z_{Production}$	5000 m	Assumption
	$z_{Injection}$	5000 m	Assumption

	Type well	Deviated	Assumption
	Type pump	LSP/ESP	Assumption
	R	1500 m	Assumption
Power plant	$\dot{m}_{TW}$	120 $kg\ /\ s$	Assumption
	ΔT^{min}	5 K	Assumption
	$T_{air,in}$	15 °C	Assumption
	Working medium	Isobutane	Assumption
	$p_{TW,in}^{Heat\ plant}$	2,2 MPa	Assumption
CHP	T_{Flow}	130 °C	Assumption
	$T_{Back\ flow}$	65 °C	Assumption
	$p_{network}$	8 bar	Assumption

A4. Further results of the investigation of the "Upper Rhine Graben"-site

Figure 15 shows all power plants with an IRR > 1%. For NPV, some power plants show low or even negative NPV. This contradiction can be explained by methodological differences. The NPV calculations are based on an interest rate of 5,42 %/a as an input parameter, while for IRR calculations, the interest rate is an output. Methodological correct, power plant configurations with an IRR lower than 5,42% don't have a positive NPV. Therefore some of the power plant configurations in Figure 15 show a negative NPV.

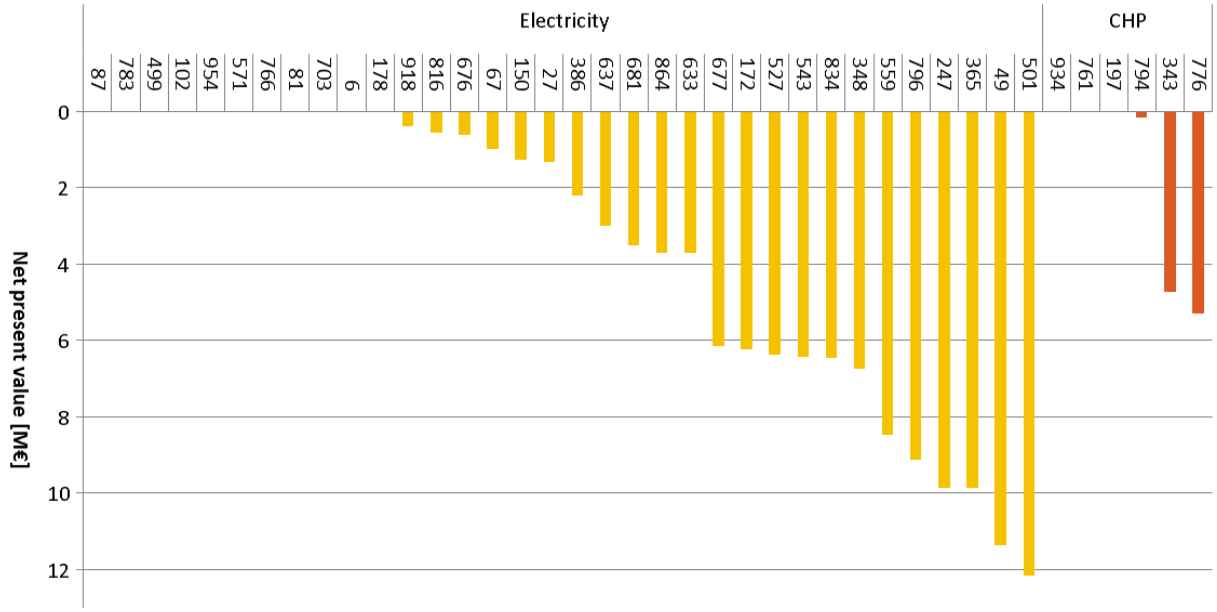

Figure 15: Comparison of pure electricity provision and CHP based on NPV (Pure electricity/CHP provision with parallel setup; baseload; ESP; $\dot{m} = 120\ kg/s$; 150 Monte-Carlo iterations; 1000 power plant configurations; hydraulic stimulation; including risk factors; with risk mitigation measures)

Figure 14, Figure 15 and Figure 16 show all power plant configurations with an IRR > 1 %/a. It becomes obvious, that none of the CHP plants is listed as an electricity plant. This suggests that the power plant configuration must be optimized on the intended purpose. The results presented in Figure 14 are based on a parallel CHP setup. For the same setup, the net power of the single power plant configurations is presented in Figure 16. On average the net power of CHP plants is roughly 50 % below the net power of pure electricity plants. Figure 16 also points out that none of the techno-economic KPI is directly correlated with the net electrical power of the plant. Power plant configuration 783 has the third highest net power but the second lowest IRR.

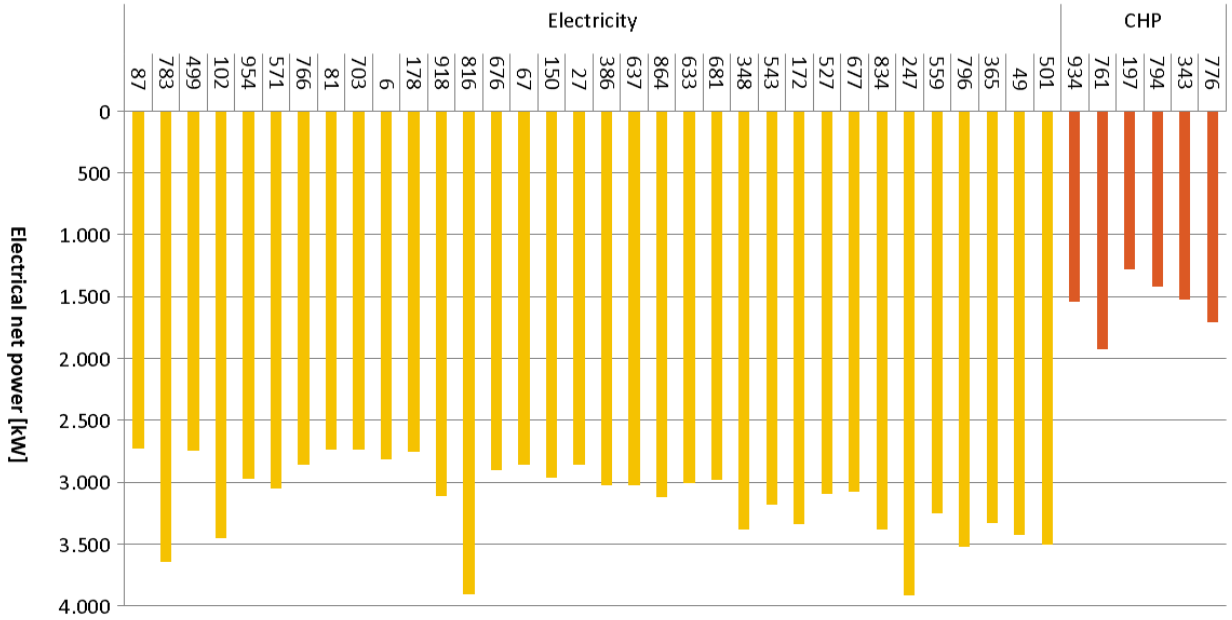

Figure 16: Net electrical power for power plant configurations selected on their IRR (Pure electricity/CHP provision with parallel setup; baseload; ESP; $\dot{m} = 120\ kg/s$; 150 Monte-Carlo iterations; 1000 power plant configurations; hydraulic stimulation; including risk factors; with risk mitigation measures)